Ecology Letters
June 2019, Volume 22 Issue 6 Pages 904-913
https://doi.org/10.1111/ele.13250
https://archimer.ifremer.fr/doc/00667/77883/

Endemic infection can shape exposure to novel pathogens: Pathogen co-occurrence networks in the Serengeti lions

Fountain-Jones Nicholas M. [1, *], Packer Craig [2], Jacquot Maude [3], Blanchet F. Guillaume [4], Terio Karen [5], Craft Meggan E. [1]

[1] Univ Minnesota, Dept Vet Populat Med, 1365 Gortner Ave, St Paul, MN 55108 ,USA.
[2] Univ Minnesota, Dept Ecol Evolut & Behav, St Paul, MN 55408 ,USA.
[3] INRA, EPIA, UMR346, Epidemiol Malad Anim & Zoonot, F-63122 St Genes Champanelle, France.
[4] Univ Sherbrooke, Dept Biol, 2500 Blvd Univ, Sherbrooke, PQ J1K 2R1, Canada.
[5] Univ Illinois, Zool Pathol Program, Urbana, IL 61801 ,USA.

* Corresponding author : Nicholas M. Fountain-Jones, email address : nfj@umn.edu

Abstract :

Pathogens are embedded in a complex network of microparasites that can collectively or individually alter disease dynamics and outcomes. Endemic pathogens that infect an individual in the first years of life, for example, can either facilitate or compete with subsequent pathogens thereby exacerbating or ameliorating morbidity and mortality. Pathogen associations are ubiquitous but poorly understood, particularly in wild populations. We report here on 10 years of serological and molecular data in African lions, leveraging comprehensive demographic and behavioural data to test if endemic pathogens shape subsequent infection by epidemic pathogens. We combine network and community ecology approaches to assess broad network structure and characterise associations between pathogens across spatial and temporal scales. We found significant non-random structure in the lion-pathogen co-occurrence network and identified both positive and negative associations between endemic and epidemic pathogens. Our results provide novel insights on the complex associations underlying pathogen co-occurrence networks.

Keywords : Babesia, calicivirus, canine distemper virus, co-infection, community assembly, coronavirus, feline immunodeficiency virus, parvovirus

Introduction

Identifying and determining the nature of interactions between multiple pathogens is increasingly considered critical to understanding infectious disease dynamics (e.g., Pedersen & Fenton 2007; Graham 2008; Telfer *et al.* 2010; Johnson *et al.* 2015; Gorsich *et al.* 2018). Individuals are often co-infected by a diverse infra-community of pathogens, and interactions between pathogens can both alter infection patterns (Cattadori *et al.* 2008; Lass *et al.* 2013; Susi *et al.* 2015) and influence disease outcomes (Moss *et al.* 2008; Munson *et al.* 2008; Knowles 2011; Wejse *et al.* 2015). Pathogens infecting individuals in the first years of life may impact infection by subsequent pathogens (Fenton 2008; Randall *et al.* 2013; Rynkiewicz *et al.* 2015; Aivelo & Norberg 2018; Budischak *et al.* 2018). For example, endemic pathogens that compete for the same resources as epidemic pathogens and can reduce the likelihood of infection (Randall *et al.* 2013) or, conversely, facilitate infection via immune suppression (e.g., Geldmacher & Koup 2012). The sequence in which pathogens infect an individual or 'priority effects' have been experimentally shown to be important in shaping co-infection dynamics in a variety of systems (e.g., Hoverman *et al.* 2013; Halliday *et al.* 2017), yet are rarely demonstrated in non-experimental contexts. How priority effects and pathogen traits (e.g., transmission mode) affect the nature and frequency of associations between endemic and epidemic pathogens, ultimately

shaping pathogen infra-communities is a knowledge gap that has significant consequences for understanding patterns of infection (Munson *et al.* 2008; Telfer *et al.* 2010; Ezenwa & Jolles 2015; Halliday *et al.* 2017).

Quantifying associations between pathogens from observational data and inferring interactions from these patterns, however, is a methodological challenge (Fenton *et al.* 2014). Discriminating between positive (i.e., two pathogens are more likely to occur together) or negative associations (i.e., two pathogens are less likely to occur together) between pathogens in populations is complicated by the short time window that a pathogen is shedding (and thus detectable with molecular methods) and by potentially confounding host immune environments (Tompkins *et al.* 2011). This is particularly the case for microparasites where pathogen detection often relies on serology, and, thus, without resampling the same individual, the precise timing of exposure cannot be estimated. Detection of pathogens that form chronic infections may be more straightforward as the infection is active for longer periods, but deducing pathogen associations is difficult without extensive longitudinal data (Fenton *et al.* 2014; Hellard *et al.* 2015). Identifying whether two pathogens are associated due to host-habitat preferences, the increasing likelihood of exposure with age, or are a product of a negative (e.g., competition) or positive (e.g., facilitation) interactions is methodologically challenging (Poulin 2007; Johnson & Buller 2011; Fenton *et al.* 2014; Hellard *et al.* 2015; Clark *et al.* 2016). Identifying associations that could represent candidate interactions based on observational data can not only provide a basis for experiments to test potential interactions but also provide novel insights into pathogen infra-community dynamics.

Detecting associations between pathogens is also likely to depend on taxonomic and spatial scales that are seldom considered (Araújo & Rozenfeld 2014; Stutz *et al.* 2018). Studies commonly aggregate pathogen data to genus level, but associations between pathogens can be subtype or genotype-specific (e.g., Wejse *et al.* 2015; Benesh & Kalbe 2016; Brook *et al.* 2017). For example, individuals infected with human immunodeficiency virus subtype 1 (HIV-1) are four times more likely to become co-infected with tuberculosis compared to individuals with HIV-2 (Wejse *et al.* 2015). Beyond subtype or genus, genotype-specific associations have been demonstrated in snails infected by trematodes (Louhi et al. 2015) and in rodents infected by

Bartonella bacteria (Brook et al. 2017). Infra-community dynamics are also likely to vary with spatiotemporal scale. In general, associations between free-living species are more apparent at scales where interactions occur compared to broader spatiotemporal scales (Eltonian noise hypothesis; Peterson *et al.* 2011; Araújo & Rozenfeld 2014), but it is unclear if this is true for pathogens. Nonetheless, for cross-sectional datasets, important patterns may be missed unless multiple spatio-temporal scales are considered (Ovaskainen *et al.* 2017). To overcome these challenges, analytical approaches that can quantify associations between pathogens whilst controlling for potential confounding factors are required to assess the role of associations in shaping pathogen infra-communities.

Recent applications of network theory to parasite community ecology provide an opportunity to move beyond the pairwise associations between two pathogens (Clark *et al.* 2016; Aivelo & Norberg 2018; Stutz *et al.* 2018). Network measures have frequently been used to study food webs but are increasingly applied to pathogen infra-communities where nodes are pathogens, and edges represent pathogen co-occurrences within the host (Vaumourin *et al.* 2015). Networks are modular if pathogens co-occur more frequently in particular groups, 'nested' if pathogens frequently share interaction partners across the network, or 'segregated' if the inverse is true (Strona & Veech 2015; Ulrich *et al.* 2017). If, for example, networks are segregated, targeted control of one 'keystone' pathogen may lead to co-extinction of other pathogens in a module (Pedersen & Fenton 2007; Säterberg *et al.* 2013). If a network is nested, perturbations to the pathogen infra-community may spread throughout the network (Griffiths *et al.* 2014).

Although pathogen co-occurrence networks are valuable for quantifying broad structural patterns, they do not account for environmental or host factors, pathogen traits or differences in spatial or temporal scale. Joint species distribution models (JSDMs) fill this gap by simultaneously assessing environmental influences and interspecific co-occurrences across multiple scales using hierarchical Bayesian mixed models (Warton *et al.* 2015; Ovaskainen *et al.* 2017). Here we use both co-occurrence networks and JSDMs to examine the structure of pathogen-pathogen networks and quantify pathogen associations while controlling for environmental/host factors and scales. We include information on pathogen traits such as transmission mode to assess what role they played in the distribution of each pathogen. We

collate ten years of cross-sectional data on endemic and epidemic pathogens in 105 African lions (*Panthera leo*) as well as extensive host and environmental data from the Serengeti Lion Project (SLP, Packer *et al.* 2005). The SLP datasets provide a unique opportunity to understand pathogen co-occurrence networks in a wild population while controlling for group, individual and environmental characteristics. We use this data to ask the following interlinked questions at two levels of taxonomic resolution:

(I) To what degree is the pathogens' co-occurrence network of Serengeti lions nested or segregated?

(II) After accounting for environmental/host factors and spatio-temporal scale, is the type of endemic pathogen an individual is infected by early in life associated with exposure to epidemic pathogens later in life?

(III) Are there significant endemic-endemic or epidemic-epidemic pathogen co-occurrences?

Because we could not directly determine the order of infection events from cross-sectional data in isolation, we used age-prevalence relationships in combination with the natural history of each pathogen to estimate probable timing of events. We describe an analytical pathway that can assess broad network structure and quantify pathogen associations across multiple scales that can generally be applied to understand infectious disease dynamics. The co-occurrence network detects clusters of pathogen sharing amongst individuals and screens for disconnected nodes (pathogens that rarely co-occur with others), while the JSDM approach was used to quantify pathogen-pathogen associations. To assess the plausibility of these putative interactions, we compare our findings to similar mammalian pathogens in experimental studies. Detecting pathogen co-occurrences not only provides novel insights into pathogen infra-community dynamics but also helps aide surveillance efforts in the field and generate testable hypotheses that can be answered in laboratory experiments.

Methods

Pathogen data

Serological testing and quantitative PCR (qPCR) were performed to detect endemic and epidemic pathogens from blood samples taken from lions in the Serengeti National Park, Tanzania from 1984-1994. In total, 394 individuals were sampled throughout this period, but our analysis was restricted to the 105 individuals tested for the full suite of ten pathogens (Table 1: pathogen natural history; Table S1: number of individuals tested per year included in the analyses). Nomadic individuals (i.e. lions that were not resident in any pride) were excluded due to the difficulty of assigning environmental variables (see *Confounding variables* below). Serological data on canine distemper virus (CDV), feline calicivirus, parvovirus, and coronavirus has been published previously, except Rift Valley Fever (RVF) (Packer *et al.* 1999, see Table S2 for assay details). To detect RVF exposure we conducted a plaque reduction virus neutralizing test (PRNT) that quantified virus neutralizing antibodies from serum following Scott *et al.* (1986) protocol.

We used qPCR to identify nucleotides for feline immunodeficiency virus (FIV_{Ple}) and the protozoan pathogens in this study (Table 1). Three distinct subtypes of FIV_{Ple} co-circulate in Serengeti lions (Troyer *et al.* 2005, 2011; Antunes *et al.* 2008) and thus subtype specific qPCR was performed (see Troyer *et al.* 2004, 2005 for qPCR protocols). The resultant 300 base pair sequences from the *pol* gene were aligned and assigned to 21 operational taxonomic units/genotypes based on a 95% molecular similarity threshold (see Fountain-Jones *et al.* 2017 for details). Lions also commonly get infected by a rich protozoan fauna including *Babesia* and *Hepatazoon* genera. We developed quantitative PCR protocols using density gel gradient electrophoresis to identify each protozoan species (see Munson *et al.* 2008).

We categorized each pathogen as likely endemic or epidemic in the lion population: endemic pathogens were considered to be constantly circulating and often infecting the young while epidemic pathogens sweep through the population every few years infecting all age classes (Packer *et al.* 1999; Penzhorn 2006; Troyer *et al.* 2011). Many of the pathogens have been previously classified as endemic or epidemic (Packer *et al.* 1999). We supported our classification with age-prevalence plots (Fig. S1) and we plotted yearly prevalence (Fig. S2) for the pathogens not previously classified. Pathogens with a high prevalence at a young age (≤ 2 y.o.) with little fluctuation across all years and age classes were considered to be likely endemic, whereas an increasing age-prevalence relationship and high temporal variation were classified as

more likely to be epidemic in this population. Feline coronavirus can have epidemic and endemic cycles, and it is challenging to assess which form the individual was infected with from serological data, but based on age-prevalence relationships we categorized coronavirus as an endemic infection (Fig. S1). Further, we used patterns of age-prevalence to infer the potential timing of infections. As most individual lions were likely to be infected by the pathogens we considered endemic within the first two years after birth (Troyer et al. 2011, Fig. S1), we assume that endemic exposure typically occurred prior to exposure by an epidemic pathogen. We partitioned the endemic pathogen data into two sets based on taxonomic resolution (high and medium). The high taxonomic resolution dataset encompassed FIV_{Ple} genotype and *Babesia* species data, whereas the medium resolution dataset aggregated FIV_{Ple} subtype information and *Babesia* data to genus level.

Co-occurrence network

We examined pathogen co-occurrence patterns to evaluate preferential associations among pathogens. We constructed co-occurrence networks for each taxonomic resolution as well as for pathogens tested for using qPCR and by serology in cases combining both lines of diagnostic evidence led to altered network structure. To do so, we first built an m × n matrix that described presences/absences (i.e., occurrences) of both endemic and epidemic pathogens across individual lions, where m was the number of individual lions and n the number of pathogens. By multiplying it by its transpose, we then created a summary n × n co-occurrence matrix that described, for each pair of pathogens, the number of observed co-occurrences across all individual lions. Pathogens detected infrequently in this lion population were included in this analysis to help screen for pathogens disconnected in the network. The co-occurrence matrix was used to evaluate which pathogens were carried by the same individuals utilizing a modularity-based ‘‘greedy’’ approach (Clauset *et al.* 2004). Measures of modularity aim to determine the adequacy of different classification schemes in representing clusters and divisions in datasets; here, the clusters represented the co-occurrence of pathogens in individual hosts. Estimates of modularity were calculated for each possible classification by comparing the expected fraction of pathogens co-occurrence to random co-occurrences (Newman 2006). The classification with the highest modularity from all the generated classifications was selected.

We then computed a measure of network structure ($\bar{N}$) and modularity index based on node overlap and segregation (Strona & Veech 2015; Ulrich *et al.* 2017). $\bar{N}$ ranges from scaled from -1 (entirely segregated network) to 1 (entirely nested network). These analyses were performed in R using the 'igraph' and 'nos' libraries (Csárdi & Nepusz 2006; Strona & Veech 2015). The co-occurrence matrix was obtained from the incidence matrix using the `graph.incidence` and the `bipartite.projection` functions. The classification analysis was performed using the `fastgreedy.community` function in igraph (Csárdi & Nepusz 2006).

Joint species distribution modeling

Joint species distribution models (JSDMs) are a flexible multivariate extension of generalized linear mixed models that can examine how environment (and host) shape multiple species simultaneously across biological scales (Ovaskainen et al. 2017; Björk et al. 2018). JSDMs can quantify associations between species across scales using latent factor models to estimate species-species covariance for each random effect (Ovaskainen et al. 2017; Björk et al. 2018). We fitted JSDMs for both high and medium taxonomic resolution datasets, combining information on environmental and host covariates as fixed effects (see Confounding variables below for details), to the occurrence data for each of the pathogens. Pathogens detected fewer than five times were excluded from this analysis leaving ten pathogens in the medium taxonomic model and 17 in the high-resolution data set. Including pathogens with fewer than five occurrences may lead to spurious associations (Ovaskainen *et al.* 2017). We fitted all the JSDMs with Bayesian inference, using "Hierarchical Modelling of Species Communities" (Blanchet *et al.* 2018). For each analysis, we modeled the response pathogen co-occurrence matrix using a probit model based on the approach outlined in Ovaskainen *et al.* (2016). In contrast to the network approach summary, the JSDM co-occurrence matrix is a product of the pathogen-to-pathogen variance-covariance matrix estimated for each random effect (e.g., pride-year) in the model. Each random effect (and thus each estimated co-occurrence matrix) measures a component of the variation in the response that is different than the other random effects and of the set of explanatory variables (fixed effects) considered in the model. In our models, we added individual (e.g., sex and age), pride, and environmental characteristics (see Confounding variables below) as fixed effects. Individual sampled, pride-year (i.e., which pride and year the

individual was sampled in), and year-landscape (i.e., what year was the individual sampled in the Serengeti) sampled were added as random effects. As pathogen traits may shape the distribution of each pathogen (e.g., similar environmental and host variables may shape tick-borne pathogens), we included traits such as pathogen type (see Table 1) in each analysis. We utilized the default priors (described in full detail in Ovaskainen *et al.* 2017) and ran the HMSC model twice using 3 million MCMC samples (the first 300 000 of which being burn-in). Each run was carried out using a different seed. Visual inspection of MCMC traces and the Gelman-Rubin diagnostic calculated to assess convergence. In addition, we made sure that the effective sample size (ESS) of each parameter was > 200.

Confounding variables

As part of the SLP, most of the individuals in this study have been regularly observed since birth (Mosser & Packer 2009). We selected 13 predictor variables that we thought were likely to be important for pathogen exposure and thus could confound possible associations patterns (Table 2). We included variables that captured individual variability (e.g., age at sampling), and pride characteristics including environmental variables (e.g., average vegetation cover of the pride's territory; see Table 2 for measurement details).

Results

The Serengeti lions were exposed to an average of 5 pathogens (two epidemic and three endemic, SD = 1); one individual had been infected by 9 of 10 pathogens (based on medium resolution data, Fig. S3). Cubs between 1 and 2 y.o. were often already infected with an average of 4 pathogens (SD = 1), with one 1.5 y.o cub positive for 5. All lions were qPCR positive for at least one protozoan species, and 25% of them were infected by all four protozoans tested.

Pathogen co-occurrence networks are highly nested

The high taxonomic resolution summary network indicated a significantly nested architecture ($\overline{N}$ = 0.74) with relatively low modularity (modularity index = 0.393, z = 3.307, p = <0.001) with three clusters (Fig. 1a). The largest cluster (green nodes) included all of the protozoans, epidemic pathogens, and some FIV_{Ple} genotypes, whilst the remaining two clusters consisted of FIV_{Ple} genotypes (Fig. 1a). When we modeled networks based on diagnostic test, the general pattern did not substantially change, with the exception that RVF clustered separately from the other viruses detected using serology. In both network formulations, phylogenetically similar genotypes of FIV did not cluster together (Fountain-Jones *et al.* 2017, see Fig. S5). In contrast, the medium resolution network was completely nested with no modularity ($\overline{N}$ = 1, modularity index = 0, z = ∞, p = 0) and no significant clusters (Fig. 1b).

Strong associations between endemic and epidemic pathogens

After accounting for environmental, individual and pride factors and scale, the JSDM analysis identified strong associations between pathogens (Fig. 2) that were not detected in the summary co-occurrence network. Including individual, pride-year and landscape-year scales in our co-occurrence models was important as our ability to detect associations varied. At an individual and pride-year level, we detected strong associations between a small subset of epidemic and endemic pathogens. FIV_{Ple} B and *H. felis* were negatively associated with RVF (Fig. 2), and FIV_{Ple} B was also negatively associated with parvovirus (Fig. 2a/S6a). However, these associations could only be detected at medium taxonomic resolution. In contrast, at high taxonomic resolution, we identified positive associations between *B. gibsoni* and RVF that were not detected at medium-resolution.

The strongest associations between endemic and epidemic pathogens were detected at the lowest spatial-temporal resolution (landscape-year). In the high taxonomic resolution model, pathogens separated into two groups with each group having a very similar association profile. One group was characterized by positive associations between the *Babesia* species, FIV_{Ple} C2, CDV, and

parvovirus. The other group was characterized by positive associations between two FIV_{Ple} genotypes (C1 & B2), coronavirus, *H. felis* and calicivirus (Figs. 2c/S6c). There were strong negative associations between pathogens in each separate group (e.g., CDV and FIV_{Ple} C1). Generally, the same associations held in the medium taxonomic resolution models (Fig. 2c/S6c), but with exceptions. For example, FIV_{Ple} C1 and C2 had opposing association profiles, but as FIV_{Ple} C1 had a higher prevalence (Fig. S7), C1 had the same overall association profile as FIV_{Ple} C.

Associations between epidemic pathogens were rare. At the year-level, we detected positive associations between CDV and parvovirus with both pathogens negatively associated with calicivirus (Fig. 2c/S6c). In contrast, associations between the endemic pathogens were common, but the nature of the associations also differed at each taxonomic scale. For example, in the medium resolution model, we detected a positive association between *H. felis* and FIV_{Ple} C not found in the high-resolution model indicating that FIV_{Ple} subtype, but not genotype, was important for this association (Fig. 2b/S6b). Strikingly, we found that FIV_{Ple} subtypes had contrasting association profiles. At the individual level, FIV_{Ple} B and C were negatively associated with each other, and FIV_{Ple} C was positively associated with coronavirus, while FIV_{Ple} B was negatively associated with coronavirus (Fig. 2a/S6a). Both high and medium taxonomic resolution JSDMs had reasonable explanatory power (Tjur R^2 = 0.381 & 0.330, respectively). In both models, the landscape and host factors that explained the distribution of each pathogen were not predicted well by pathogen traits (See Fig. S8). See Fig. 3 for a summary of all of the associations detected across scales from our cross-sectional data and Figs. S9/10 for model details.

Discussion

Here we demonstrate non-random associations in the pathogens infecting wild African lions, with both negative and positive associations detected between endemic and epidemic pathogens. While there was minimal structure in the summary co-occurrence network (Fig. 1a), we uncovered structure after accounting for scale and controlling for potentially confounding environmental and host variables and scale (Fig. 2). Using age-prevalence relationships we could

assess the likely order of infection using cross-sectional data. We found that the particular endemic pathogen an individual is infected by as a cub may have consequences for which novel epidemic pathogen the individual is infected with later in life (Fig. 3). We emphasize that the approach used here can start to untangle pathogen infra-community relationships and identify potential endemic-epidemic associations in wild populations. These can then be compared with knowledge of pathogen pathogenesis and validated *in-vitro* in a laboratory setting. While clinical or laboratory studies of co-infection in lions are rare for good reason, the associations we found have clear precedence in similar pathogens co-infecting humans and represent plausible interactions. Our results not only provide new insights on pathogen community structure in the Serengeti lions but also provide a valuable framework for exploring pathogen co-occurrence networks and infra-community dynamics.

Co-occurrence networks were highly nested with relatively low modularity, particularly at a medium taxonomic resolution. Nonetheless, RVF did cluster separately from the other pathogens tested via serology which potentially indicates that RVF, unlike the other epidemic viruses, has a distinct epidemic cycle with most of the interacting partners being more chronic pathogens. This is supported by the unique association profile detected in our JSDM analysis and is intuitive given that RVF is the only mosquito-borne pathogen that we sampled. Even though we sampled pathogens considered important for lion health, we lacked data on other potentially pathogenic bacteria, helminths, and fungi that the lions were exposed to or potentially infected by. Further, symbiont interactions can also be important in shaping pathogen dynamics (e.g., Halliday *et al.* 2017) and could be considered in pathogen infra-community studies. These additional taxa may lead to further segregation in the network, as larger and more diverse networks typically show increased modularity and segregation (Thebault & Fontaine 2010; Sauve *et al.* 2014). Expanding sampling to construct a more complete microbe and macroparasite network would also capture a broader array of potentially facilitative and competitive associations (Ezenwa 2016; Aivelo & Norberg 2018).

After accounting for environment, host and scale, we found that the endemic pathogens were strongly associated with the epidemic pathogens and, based on mammalian lab-based experiments, suggest that these patterns represent plausible interactions between pathogens. For example, we detected negative associations between endemic pathogens (FIV_{Ple} B and *H. felis*) and RVF after accounting for differences between individuals. Coinfections between bunyaviruses like RVF and retroviruses are likely common in humans and wildlife, though there are surprisingly few studies addressing the topic. In contrast, relationships between dengue virus (a flavivirus) and HIV are relatively well understood. Flaviviruses and HIV share similar immune receptors that can inhibit HIV replication and the molecular machinery used to do so may be a viable way to control HIV infection (e.g., Xiang *et al.* 2009). Given the overall structural similarity of flaviviruses and bunyaviruses (Hernandez *et al.* 2014), it is possible that a similar mechanism underlies the association in lions between RVF and FIV_{Ple} that we observed, although we show that this association was subtype specific. If this was true, RVF might inhibit FIV_{Ple} B infection— counter to our assumption that endemic pathogens in our system infected each individual first (Fig. 3).

The greatest number of associations between epidemic and endemic pathogens were detected when we included differences across years (year-landscape scale) in our analysis. These associations could represent plausible facilitative or competitive interactions. CDV and *Babesia* are well known to interact with high levels of *Babesia* infection magnifying the impacts of consequent T cell depletion caused by CDV infection leading to mortality of nearly 40% of the lion population in 1994 (Munson *et al.* 2008). We found that all tick-borne hemoparasites showed positive associations with CDV including *B. leo* (with insert) despite its low prevalence in 1993/4 (Fig. S9). Parvovirus was also positively associated with CDV, but this was likely due to similarities in timings of epidemics with a parvovirus epidemic in 1992 just before the 1994 CDV epidemic (Packer *et al.* 1999). Parvoviruses are also immune suppressive, and so the timing of the parvovirus outbreak may also have contributed to the CDV/*Babesia*-induced mortality. The general negative relationship between FIV_{Ple} C and CDV/*Babesia* supports the theory that individuals infected by subtype C were more likely to die in the consequent *Babesia*/CDV

outbreak (Troyer *et al.* 2011). Thus, this negative association may not be due to competition between pathogens but rather to mortality.

Our approach detected strong associations between the endemic pathogens also. For example, there were opposing associations between the FIV_{Ple} subtypes and coronavirus (Fig. 2). Negative associations between retroviruses and coronaviruses are rarely reported, yet there are plausible molecular pathways. HIV-1 and human coronaviruses (HCoV) share remarkably similar binding receptors (Chan *et al.* 2006) and some mild HCoV strains are even considered a viable vaccine against HIV (Eriksson *et al.* 2006). This may explain the negative association we detected for FIV_{Ple} B and coronavirus but does not explain the positive association between FIV_{Ple} C and coronavirus we detected across scales. The mechanism driving FIV_{Ple} subtype specific relationships with coronaviruses are unclear, and as coronaviruses infecting lions are also likely to be genetically diverse, examining the genetic structure of coronavirus may help untangle these associations further. In contrast, competitive associations between HIV strains are well characterized with HIV-1 found to outcompete HIV-2 for blood resources (Ariën *et al.* 2005). For FIV_{Ple}, even though co-infection is relatively common (Troyer *et al.* 2011) competition between subtypes could be important as there is anecdotal cell culture evidence that FIV_{Ple} B can propagate more rapidly than FIV_{Ple} C (Melody Roelke, unpublished data).

There were also contrasting associations between the protozoan species. For example, the distribution of *B. felis* was not shaped by any other protozoan and in general, had a narrow association profile (Fig. 2), unlike the other *Babesia* species. For the individuals co-infected by protozoans, associations involving *B. felis* were also common, whereas co-infections involving *H. felis* and the other *Babesia* species varied in prevalence and composition (Fig. S9). Even though *B. gibsoni* and *B. felis* show similar age prevalence profiles (Fig. S1), the prevalence of *B. felis* over time was relatively stable compared to the other protozoa (Fig. S10). Differences in the host range for individual *Babesia* species and potential host differences in virulence may partially explain these patterns. For example, *B. felis* has only ever been detected in felids, whereas *B. gibsoni* has a much broader host range including canids (Penzhorn 2006). Generalist

pathogens may have greater pathogenicity as there can be reduced selective restraint on virulence particularly in 'dead end' hosts (Woolhouse *et al.* 2001). If more pathogenic species are more likely to interact with other pathogens compared to less virulent pathogens is an open question in disease ecology. Importantly, patterns like these would be missed without incorporating high-resolution pathogen data.

There are, however, limitations to this approach. The inability to distinguish mortality or correlated exposure (i.e., an individual is infected by multiple pathogens in the same transmission event) from negative associations is one of them, and careful interpretation of negative associations is necessary. Incorporating approaches such as structural equation models that explicitly include potential mechanisms that underlie candidate pathogen associations (Carver *et al.* 2015) could be a valuable additional step in future pathogen network studies. Another weakness is the inability to estimate the timing of these infections more precisely. For example, the negative association between RVF and *H. felis* could be due to temporal differences when ticks and mosquitoes emerge after rains. Years with higher rainfall increase mosquito abundance thus increasing RVF prevalence (Fig. S2) whereas ticks emerge *en masse* when rains follow a dry period potentially increasing *H. felis* prevalence (Munson *et al.* 2008). As rainfall was calibrated to the year of sampling rather than the age of infection (which could differ) the JSDM approach could not capture this variation. Studies using longitudinal data to quantify associations using a similar framework to ours (e.g., Telfer *et al.* 2010; Henrichs *et al.* 2016) will be beneficial as they are likely to provide more robust estimates of the order of infection in wild populations. Furthermore, we cannot quantify the importance of these associations in shaping pathogen distribution across scales compared to processes such as host density. Lastly, incorporating immune function and host resources in both the summary network and JSDM analyses are likely to provide mechanistic insight into pathogen network structure (Griffiths *et al.* 2014). Higher resolution pathogen traits, such as duration of infection, are likely to provide further mechanistic insight into how and why pathogens co-occur as they do in free-living communities (Ulrich *et al.* 2017). However, given the daunting complexity of pathogen infra-community dynamics, our two-step approach can assess broad network structure and identify useful candidate interactions between pathogens thereby reducing some of this complexity.

The high frequency of co-occurrence and co-infection in lions – and the potential for specific associations to cause population decline – highlights the importance of understanding pathogen associations. The summary lion pathogen co-occurrence network was highly connected with both positive and negative associations between endemic and epidemic pathogens. Our findings indicate that the lion pathogen infra-community is influenced by a number of ecological factors and associations between pathogens. We identify useful associations between pathogens thereby reducing some of this complexity. More broadly, our work demonstrates how different network approaches can be combined to gain insights into the ecological factors underlying pathogen associations and how this can be applied to the study of pathogen communities in wildlife populations. In addition to these biological insights, the study highlights several critical areas for methodological improvement that can currently limit robust inference of pathogen associations from cross-sectional serological and qPCR data. Addressing these limitations is timely, given the ongoing threat of wildlife population decline, creating a need to integrate better molecular, ecological and network information for disease control.

Acknowledgements

N.M F-J. and MEC were funded by National Science Foundation (DEB-1413925 and 1654609), the University of Minnesota' Office of the Vice President for Research and Academic Health Center Seed Grant, and the Cooperative State Research Service, U.S. Department of Agriculture, under Project No. MIN-62-098. We thank the three anonymous reviewers for their constructive feedback on this paper. We also thank Dr. Linda Munson who led the CDV-*Babesia* work and Professor CJ Peters for performing the RVF virus neutralization tests.

References

Aivelo, T. & Norberg, A. (2018). Parasite-microbiota interactions potentially affect intestinal communities in wild mammals. *J. Anim. Ecol.*, 87, 438–447.

Antunes, A., Troyer, J.L., Roelke, M.E., Pecon-Slattery, J., Packer, C., Winterbach, C., *et al.* (2008). The evolutionary dynamics of the lion *Panthera leo* revealed by host and viral population genomics. *PLoS Genet.*, 4, e1000251.

Araújo, M.B. & Rozenfeld, A. (2014). The geographic scaling of biotic interactions. *Ecography (Cop.).*, 37, 406–415.

Ariën, K.K., Abraha, A., Quiñones-Mateu, M.E., Kestens, L., Vanham, G. & Arts, E.J. (2005). The replicative fitness of primary human immunodeficiency virus type 1 (HIV-1) group M, HIV-1 group O, and HIV-2 isolates. *J. Virol.*, 79, 8979–90.

Benesh, D.P. & Kalbe, M. (2016). Experimental parasite community ecology: intraspecific variation in a large tapeworm affects community assembly. *J. Anim. Ecol.*, 85, 1004–1013.

Björk, J.R., Hui, F.K.C., O'Hara, R.B. & Montoya, J.M. (2018). Uncovering the drivers of host-associated microbiota with joint species distribution modelling. *Mol. Ecol.*, 27, 2714–2724.

Blanchet, F.G., Tikhonov, G. & Norberg, A. (2018). HMSC: Hierarchical Modelling of Species Community. R package version 2.2-1.

Brook, C.E., Bai, Y., Yu, E.O., Ranaivoson, H.C., Shin, H., Dobson, A.P., *et al.* (2017). Elucidating transmission dynamics and host-parasite-vector relationships for rodent-borne *Bartonella* spp. in Madagascar. *Epidemics*, 20, 56–66.

Budischak, S.A., Wiria, A.E., Hamid, F., Wammes, L.J., Kaisar, M.M.M., van Lieshout, L., *et al.* (2018). Competing for blood: the ecology of parasite resource competition in human malaria-helminth co-infections. *Ecol. Lett.*, 21, 536–545.

Carver, S., Beatty, J.A., Troyer, R.M., Harris, R.L., Stutzman-Rodriguez, K., Barrs, V.R., *et al.* (2015). Closing the gap on causal processes of infection risk from cross-sectional data: structural equation models to understand infection and co-infection. *Parasit. Vectors*, 8, 658.

Cattadori, I.M., Boag, B. & Hudson, P.J. (2008). Parasite co-infection and interaction as drivers of host heterogeneity. *Int. J. Parasitol.*, 38, 371–380.

Chan, V.S.F., Chan, K.Y.K., Chen, Y., Poon, L.L.M., Cheung, A.N.Y., Zheng, B., *et al.* (2006). Homozygous L-SIGN (CLEC4M) plays a protective role in SARS coronavirus infection. *Nat. Genet.*, 38, 38–46.

Clark, N.J., Wells, K., Dimitrov, D. & Clegg, S.M. (2016). Co-infections and environmental conditions drive the distributions of blood parasites in wild birds. *J. Anim. Ecol.*, 85, 1461–1470.

Clauset, A., Newman, M.E.J. & Moore, C. (2004). Finding community structure in very large networks. *Phys. Rev. E*, 70.

Csárdi, G. & Nepusz, T. (2006). The igraph software package for complex network research. *InterJournal Complex Syst.*, 1695.

Eriksson, K.K., Makia, D., Maier, R., Ludewig, B. & Thiel, V. (2006). Towards a coronavirus-based HIV multigene vaccine. *Clin. Dev. Immunol.*, 13, 353–60.

Ezenwa, V.O. (2016). Helminth-microparasite co-infection in wildlife: lessons from ruminants, rodents and rabbits. *Parasite Immunol.*, 38, 527–534.

Ezenwa, V.O. & Jolles, A.E. (2015). Opposite effects of anthelmintic treatment on microbial infection at individual versus population scales. *Science*, 347, 175–7.

FAO & IIASA. (2009). *Harmonized world soil database*. Food and Agriculture Organization.

Fenton, A. (2008). Worms and germs: the population dynamic consequences of microparasite-macroparasite co-infection. *Parasitology*, 135, 1545–1560.

Fenton, A., Knowles, S.C.L., Petchey, O.L. & Pedersen, A.B. (2014). The reliability of observational approaches for detecting interspecific parasite interactions: comparison with experimental results. *Int. J. Parasitol.*, 44, 437–445.

Fountain-Jones, N.M., Packer, C., Troyer, J.L., VanderWaal, K., Robinson, S., Jacquot, M., *et al.* (2017). Linking social and spatial networks to viral community phylogenetics reveals subtype-specific transmission dynamics in African lions. *J. Anim. Ecol.*, 86, 1469–1482.

Geldmacher, C. & Koup, R.A. (2012). Pathogen-specific T cell depletion and reactivation of opportunistic pathogens in HIV infection. *Trends Immunol.*, 33, 207–14.

Gorsich, E.E., Etienne, R.S., Medlock, J., Beechler, B.R., Spaan, J.M., Spaan, R.S., *et al.* (2018). Opposite outcomes of coinfection at individual and population scales. *Proc. Natl. Acad. Sci.*

U. S. A., 115, 7545–7550.

Graham, A.L. (2008). Ecological rules governing helminth-microparasite coinfection. *Proc. Natl. Acad. Sci. U. S. A.*, 105, 566–70.

Griffiths, E.C., Pedersen, A.B., Fenton, A. & Petchey, O.L. (2014). Analysis of a summary network of co-infection in humans reveals that parasites interact most via shared resources. *Proceedings. Biol. Sci.*, 281, 20132286.

Halliday, F.W., Umbanhowar, J. & Mitchell, C.E. (2017). Interactions among symbionts operate across scales to influence parasite epidemics. *Ecol. Lett.*, 20, 1285–1294.

Hellard, E., Fouchet, D., Vavre, F. & Pontier, D. (2015). Parasite–parasite interactions in the wild: How to detect them? *Trends Parasitol.*, 31, 640–652.

Henrichs, B., Oosthuizen, M.C., Troskie, M., Gorsich, E., Gondhalekar, C., Beechler, B.R., *et al.* (2016). Within guild co-infections influence parasite community membership: a longitudinal study in African Buffalo. *J. Anim. Ecol.*, 85, 1025–1034.

Hernandez, R., Brown, D.T. & Paredes, A. (2014). Structural differences observed in arboviruses of the alphavirus and flavivirus genera. *Adv. Virol.*, 2014, 259382.

Hoverman, J.T., Hoye, B.J. & Johnson, P.T.J. (2013). Does timing matter? How priority effects influence the outcome of parasite interactions within hosts. *Oecologia*, 173, 1471–1480.

Johnson, P.T.J. & Buller, I.D. (2011). Parasite competition hidden by correlated coinfection: using surveys and experiments to understand parasite interactions, 92, 535–541.

Johnson, P.T.J., de Roode, J.C. & Fenton, A. (2015). Why infectious disease research needs community ecology. *Science*, 349, 1259504–1259504.

Knowles, S.C.L. (2011). The effect of helminth co-infection on malaria in mice: A meta-analysis. *Int. J. Parasitol.*, 41, 1041–1051.

Lass, S., Hudson, P.J., Thakar, J., Saric, J., Harvill, E., Albert, R., *et al.* (2013). Generating super-shedders: co-infection increases bacterial load and egg production of a gastrointestinal helminth. *J. R. Soc. Interface*, 10, 20120588.

570 Moss, W.J., Fisher, C., Scott, S., Monze, M., Ryon, J.J., Quinn, T.C., *et al.* (2008). HIV Type 1
571 infection is a risk factor for mortality in hospitalized Zambian children with measles. *Clin.*
572 *Infect. Dis.*, 46, 523–527.

573 Mosser, A., Fryxell, J.M., Eberly, L. & Packer, C. (2009). Serengeti real estate: density vs.
574 fitness-based indicators of lion habitat quality. *Ecol. Lett.*, 12, 1050–1060.

575 Mosser, A. & Packer, C. (2009). Group territoriality and the benefits of sociality in the African
576 lion, Panthera leo. *Anim. Behav.*, 78, 359–370.

577 Munson, L., Terio, K.A., Kock, R., Mlengeya, T., Roelke, M.E., Dubovi, E., *et al.* (2008).
578 Climate extremes promote fatal co-infections during canine distemper epidemics in African
579 lions. *PLoS One*, 3, e2545.

580 Newman, M.E.J. (2006). Community structure in social and biological networks. *Proc. Natl.*
581 *Acad. Sci. U. S. A.*, 99, 7821–6.

582 Ovaskainen, O., Abrego, N., Halme, P. & Dunson, D. (2016). Using latent variable models to
583 identify large networks of species-to-species associations at different spatial scales.
584 *Methods Ecol. Evol.*, 7, 549–555.

585 Ovaskainen, O., Tikhonov, G., Norberg, A., Guillaume Blanchet, F., Duan, L., Dunson, D., *et al.*
586 (2017). How to make more out of community data? A conceptual framework and its
587 implementation as models and software. *Ecol. Lett.*, 20, 561–576.

588 Packer, C., Altizer, S., Appel, M., Brown, E., Martenson, J., O'Brien, S.J., *et al.* (1999). Viruses
589 of the Serengeti: patterns of infection and mortality in African lions. *J. Anim. Ecol.*, 68,
590 1161–1178.

591 Packer, C., Hilborn, R., Mosser, A., Kissui, B., Borner, M., Hopcraft, G., *et al.* (2005).
592 Ecological change, group territoriality, and population dynamics in Serengeti lions. *Science*,
593 307, 390–3.

594 Pedersen, A.B. & Fenton, A. (2007). Emphasizing the ecology in parasite community ecology.
595 *Trends Ecol. Evol. Evol.*, 22, 133–9.

Penzhorn, B.L. (2006). Babesiosis of wild carnivores and ungulates. *Vet. Parasitol.*, 138, 11–21.

Peterson, A.T. (Andrew T., Soberon, J., Pearson, R., Anderson, R., Martinez-Meyer, M., Nakamura, M., *et al.* (2011). *Ecological niches and geographic distributions*. Princeton University Press, Princeton.

Poulin, R. (2007). Are there general laws in parasite ecology? *Parasitology*, 134, 763–766.

Randall, J., Cable, J., Guschina, I.A., Harwood, J.L. & Lello, J. (2013). Endemic infection reduces transmission potential of an epidemic parasite during co-infection. *Proceedings. Biol. Sci.*, 280, 20131500.

Reed, D.N., Anderson, T.M., Dempewolf, J., Metzger, K. & Serneels, S. (2009). The spatial distribution of vegetation types in the Serengeti ecosystem: the influence of rainfall and topographic relief on vegetation patch characteristics. *J. Biogeogr.*, 36, 770–782.

Rynkiewicz, E.C., Pedersen, A.B. & Fenton, A. (2015). An ecosystem approach to understanding and managing within-host parasite community dynamics. *Trends Parasitol.*, 31, 212–221.

Säterberg, T., Sellman, S. & Ebenman, B. (2013). High frequency of functional extinctions in ecological networks. *Nature*, 499, 468–470.

Sauve, A.M.C., Fontaine, C. & Thébault, E. (2014). Structure-stability relationships in networks combining mutualistic and antagonistic interactions. *Oikos*, 123, 378–384.

Scott, R.M., Feinsod, F.M., Allam, I.H., Ksiazek, T.G., Peters, C.J., Botros, B.A.M., *et al.* (1986). Serological tests for detecting rift valley fever viral antibodies in sheep from the Nile Delta. *J. Clin. Microbiol.*, 24, 612–614.

Sinclair, A.R.E., Metzger, K.L., Fryxell, J.M., Packer, C., Byrom, A.E., Craft, M.E., *et al.* (2013). Asynchronous food-web pathways could buffer the response of Serengeti predators to El Niño Southern Oscillation. *Ecology*, 94, 1123–1130.

Strona, G. & Veech, J.A. (2015). A new measure of ecological network structure based on node overlap and segregation. *Methods Ecol. Evol.*, 6, 907–915.

Stutz, W.E., Blaustein, A.R., Briggs, C.J., Hoverman, J.T., Rohr, J.R. & Johnson, P.T.J. (2018).

Using multi-response models to investigate pathogen coinfections across scales: Insights from emerging diseases of amphibians. *Methods Ecol. Evol.*, 9, 1109–1120.

Susi, H., Barrès, B., Vale, P.F., Laine, A.-L., Mideo, N., Alizon, S., *et al.* (2015). Co-infection alters population dynamics of infectious disease. *Nat. Commun.*, 6, 5975.

Telfer, S., Lambin, X., Birtles, R., Beldomenico, P., Burthe, S., Paterson, S., *et al.* (2010). Species interactions in a parasite community drive infection risk in a wildlife population. *Science*, 330, 243–6.

Thebault, E. & Fontaine, C. (2010). Stability of ecological communities and the architecture of mutualistic and trophic networks. *Science*, 329, 853–856.

Tompkins, D.M., Dunn, A.M., Smith, M.J. & Telfer, S. (2011). Wildlife diseases: from individuals to ecosystems. *J. Anim. Ecol.*, 80, 19–38.

Troyer, J.L., Pecon-Slattery, J., Roelke, M.E., Black, L., Packer, C. & O'Brien, S.J. (2004). Patterns of feline immunodeficiency virus multiple infection and genome divergence in a free-ranging population of African lions. *J. Virol.*, 78, 3777–3791.

Troyer, J.L., Pecon-Slattery, J., Roelke, M.E., Johnson, W., VandeWoude, S., Vazquez-Salat, N., *et al.* (2005). Seroprevalence and genomic divergence of circulating strains of feline immunodeficiency virus among Felidae and Hyaenidae species. *J. Virol.*, 79, 8282–8294.

Troyer, J.L., Roelke, M.E., Jespersen, J.M., Baggett, N., Buckley-Beason, V., MacNulty, D., *et al.* (2011). FIV diversity: FIV $_{Ple}$ subtype composition may influence disease outcome in African lions. *Vet. Immunol. Immunopathol.*, 143, 338–346.

Ulrich, W., Kryszewski, W., Sewerniak, P., Puchałka, R., Strona, G. & Gotelli, N.J. (2017). A comprehensive framework for the study of species co-occurrences, nestedness and turnover. *Oikos*, 126, 1607–1616.

Vaumourin, E., Vourc'h, G., Gasqui, P., Vayssier-Taussat, M., Windsor, D., Anderson, R., *et al.* (2015). The importance of multiparasitism: examining the consequences of co-infections for human and animal health. *Parasit. Vectors*, 8, 545.

Warton, D.I., Blanchet, F.G., O'Hara, R.B., Ovaskainen, O., Taskinen, S., Walker, S.C., *et al.* (2015). So many variables: Joint modeling in community ecology. *Trends Ecol. Evol.*, 30, 766–79.

Wejse, C., Patsche, C.B., Kühle, A., Bamba, F.J.V., Mendes, M.S., Lemvik, G., *et al.* (2015). Impact of HIV-1, HIV-2, and HIV-1+2 dual infection on the outcome of tuberculosis. *Int. J. Infect. Dis.*, 32, 128–134.

Westgate, M.J. (2016). circleplot: Circular plots of distance and association matrices. R package version 0.4.

Woolhouse, M.E.J., Taylor, L.H. & Haydon, D.T. (2001). Population biology of multihost pathogens. *Science*, 292, 1109–1112.

Xiang, J., McLinden, J.H., Rydze, R.A., Chang, Q., Kaufman, T.M., Klinzman, D., *et al.* (2009). Viruses within the Flaviviridae decrease CD4 expression and inhibit HIV replication in human CD4+ cells. *J. Immunol.*, 183, 7860–9.

Table 1: Traits of both endemic and epidemic pathogens in this study.

Pathogen	**Type**	**Trans. mode**	**One host?**	**Immune sup.**	**Exposure timing?***	**Test type**
Data type	**(binary)**	**(categorical)**	**(binary)**	**(binary)**	**(binary)**	**(binary)**
EPIDEMIC						
Feline calicivirus (calicivirus) †	Virus	Direct/env	N	NE	Epidemic year	Serology
Canine distemper virus (CDV)	Virus	Direct	N	Yes	Epidemic year	Serology
Feline panleukopenia (parvovirus)	Virus	Vertical, direct/env	N	Yes	Epidemic year	Serology
Rift valley fever (RVF)	Virus	Vector (mosquito)	N	Yes	Throughout life#	Serology
ENDEMIC						

Feline enteric coronavirus (coronavirus) †	Virus	Vector	N	U	Epidemic year	Serology
B. gibsoni	Protozoa	Vector (tick)	N	NE	< 2 y.o	qPCR
***B. leo* with insertion**	Protozoa	Vector(tick)	N	NE	Throughout life	qPCR
B. felis	Protozoa	Vector (tick)	N	NE	< 2 y.o.	qPCR
Hepatozoon felis	Protozoa	Vector (tick)	N	NE	< 2 y.o.	qPCR
Feline immunodeficiency virus FIV_{Ple} A, B, and C and FIV genotypes A1, B1-12, C1-C8	Virus	Vertical/ direct	Y	Yes	< 2 y.o.	qPCR

Trans. mode : Transmission mode (all pathogens can be horizontally transmitted). Immune sup.: Pathogen can suppress the immune system. Vertical: Vertical transmission is also possible. Env: Environmentally persistent. Direct: Transmission through host contact. Immune sup.: Immune suppression.*: Likely time of exposure †: Determined by age-prevalence relationships (see *Methods* and Fig. S1) but can have endemic or epidemic variants. U: Unknown NE: No evidence. #: More likely after heavy rainfall (Fig. S2).

Table 2: Details of the individual, pride-level and environmental predictors used in the joint species distribution models to help account for potential confounding factors. All variables were calculated based on the year of sampling.

Predictor	Type	Measurement details	Data
Sex	Individual	Male or female.	SLP data
Age	Individual	Age of lion when sampled (days).	SLP data
Number of immigrations	Individual	Number of prides an individual has immigrated into prior to sampling.	SLP data
Pride or coalition male?	Individual	Was the male involved in a coalition occupying multiple prides (binary)?	SLP data

Group size	Pride	Average number of individuals in pride two years† prior to sample collection.	SLP data
Despotic	Pride	Was the pride considered despotic at time of sample collection?	SLP data
Territory size	Pride	Based on location data over a two-year period based on utilization–distribution curves with a 75% kernel.	SLP data
Territory overlap	Pride	What percentage of territory size overlapped with other prides.	SLP data
Habitat quality	Pride	Pride habitat quality score calculated across a two-year period.	(Mosser *et al*. 2009)
Number of neighbors	Pride	Number of individuals in neighboring prides. Neighboring prides had territory overlap.	SLP data
Yearly rainfall	Environmental	Yearly rainfall experienced in each pride territory based on weather stations in the plains and woodlands.	(Sinclair *et al.* 2013)
Average vegetation cover	Environmental	Average vegetation cover across the prides territory based on a 75% kernal.	(Reed *et al.* 2009)
Soil pH	Environmental	Average pH throughout the pride's territory based on a 75% kernel.	World Harmonized Soil Database (FAO & IIASA 2009).

672 * We calculated this predictor two years prior to sampling to account for differences in individual status at a
673 potential time of exposure or infection (e.g., individuals that had just immigrated into a pride when sampled were
674 considered nomads as exposure or infection was likely to have occurred previously). †: We averaged over past two
675 years to reduce the variability in pride counts as exposure was unlikely to have happened during the sampling year.

676

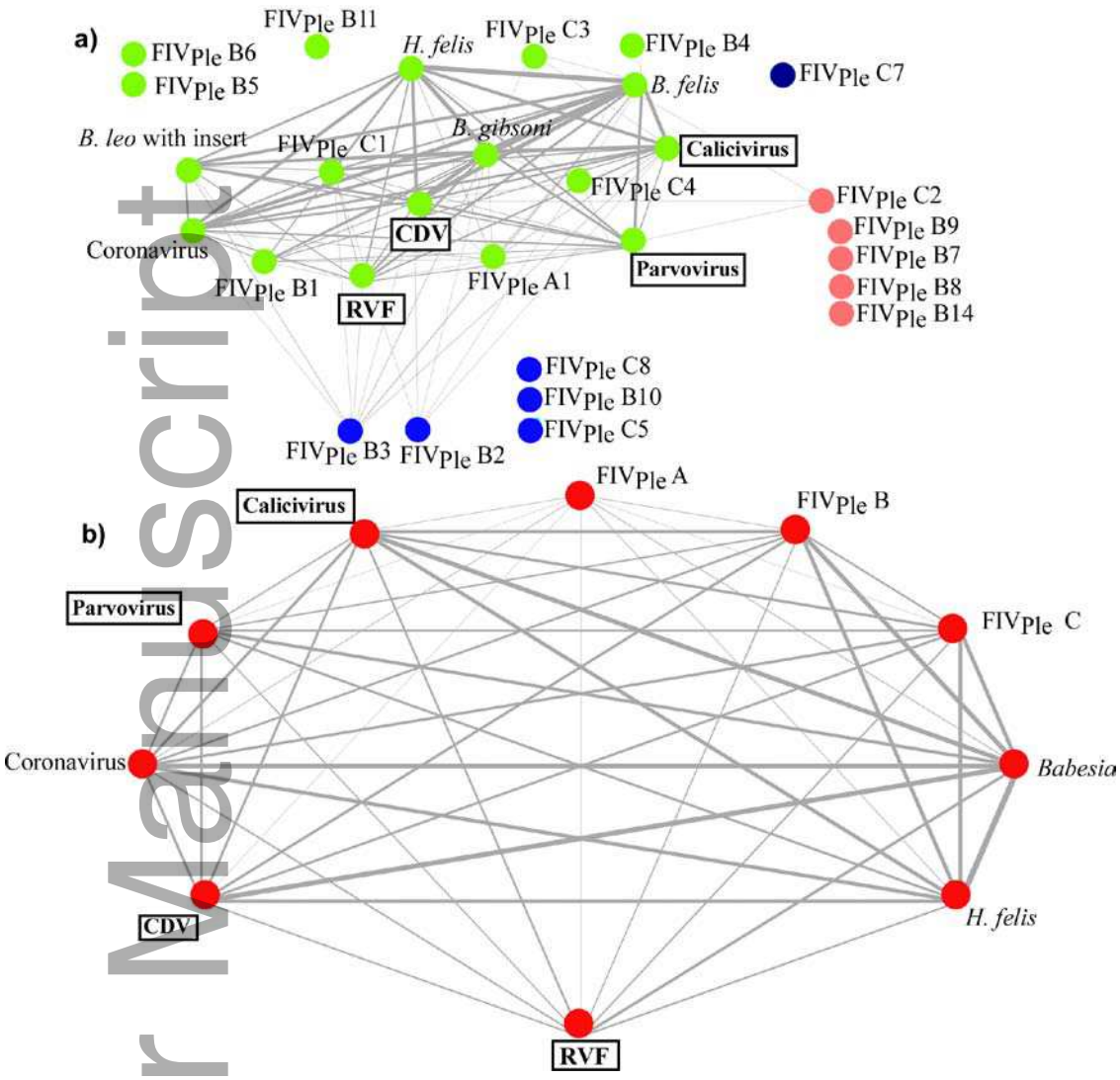

677

678 **Fig. 1:** Pathogen summary co-occurrence network for a) high taxonomic resolution and b)
679 medium taxonomic resolution data, where nodes are pathogens and edges reflect co-occurrence.
680 Edges are shown only when there were ≥ 3 co-occurrences. Node colors reflect separate clusters.
681 Edge weights are proportional to the number of co-occurrences. Pathogen labels in bold (in
682 boxes) were considered epidemic. See Fig. S4 for networks fo pathogens detected via qPCR and
683 serology separately.

684

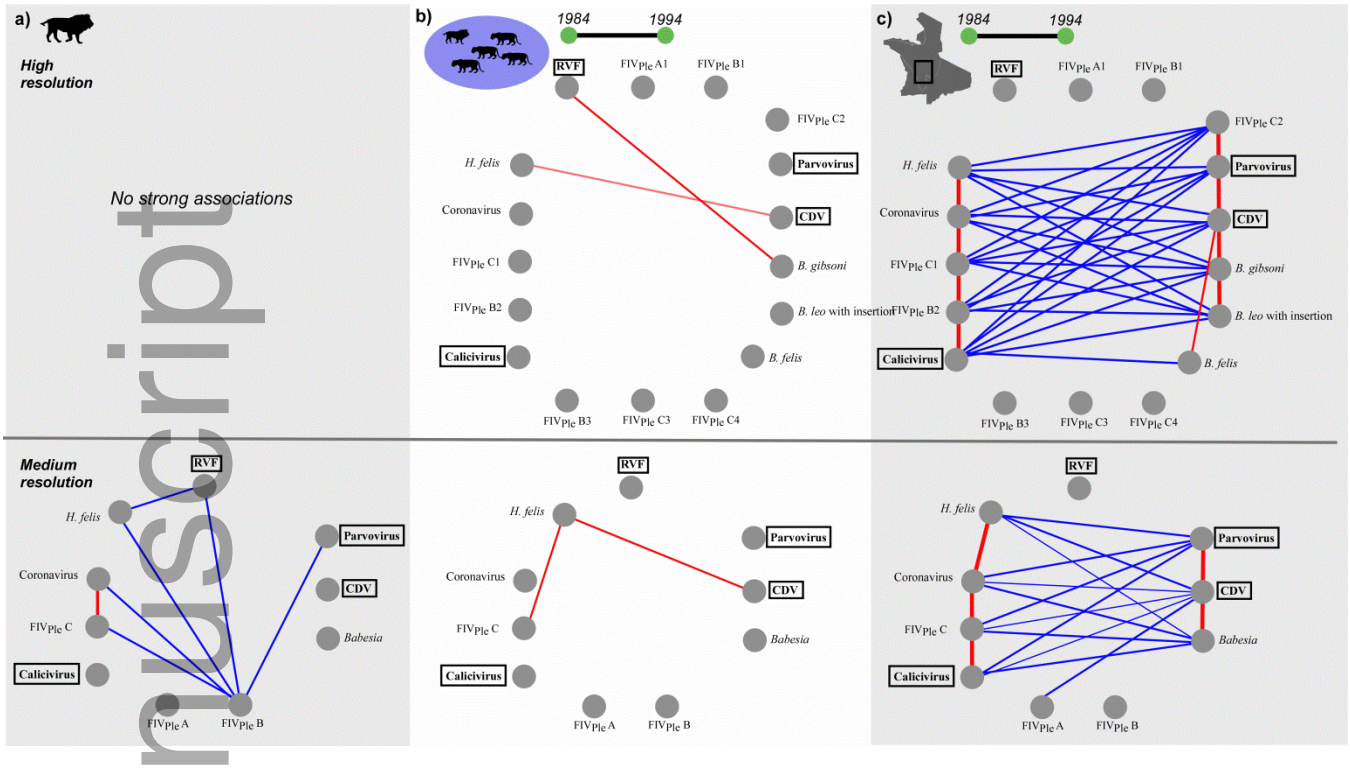

685

686 **Fig. 2:** Pathogen-pathogen associations detected at (a) individual, (b) pride-year and (c)
687 landscape-year level after controlling for individual, pride, and environmental variables in high
688 and medium taxonomic resolution models. Blue represents negative correlations and red
689 indicates positive associations. Only associations with posterior coefficient estimates ≥ 0.4 with
690 95% credible intervals that do not cross 0 are shown. The light red line indicates the assocation
691 between *H. felis* and CDV that was ≥ 0.4 in the medium resolution model but was below the
692 threshold (0.38) in the high resolution model. Pathogens in bold and in boxes are the epidemic
693 viruses (all other pathogens are likely endemic). This figure was drawn using the R package
694 'circleplot' (Westgate 2016). See Fig. S6 for association matrices and Figs. S9/S10 for covariate
695 partitioning and effect size.

696

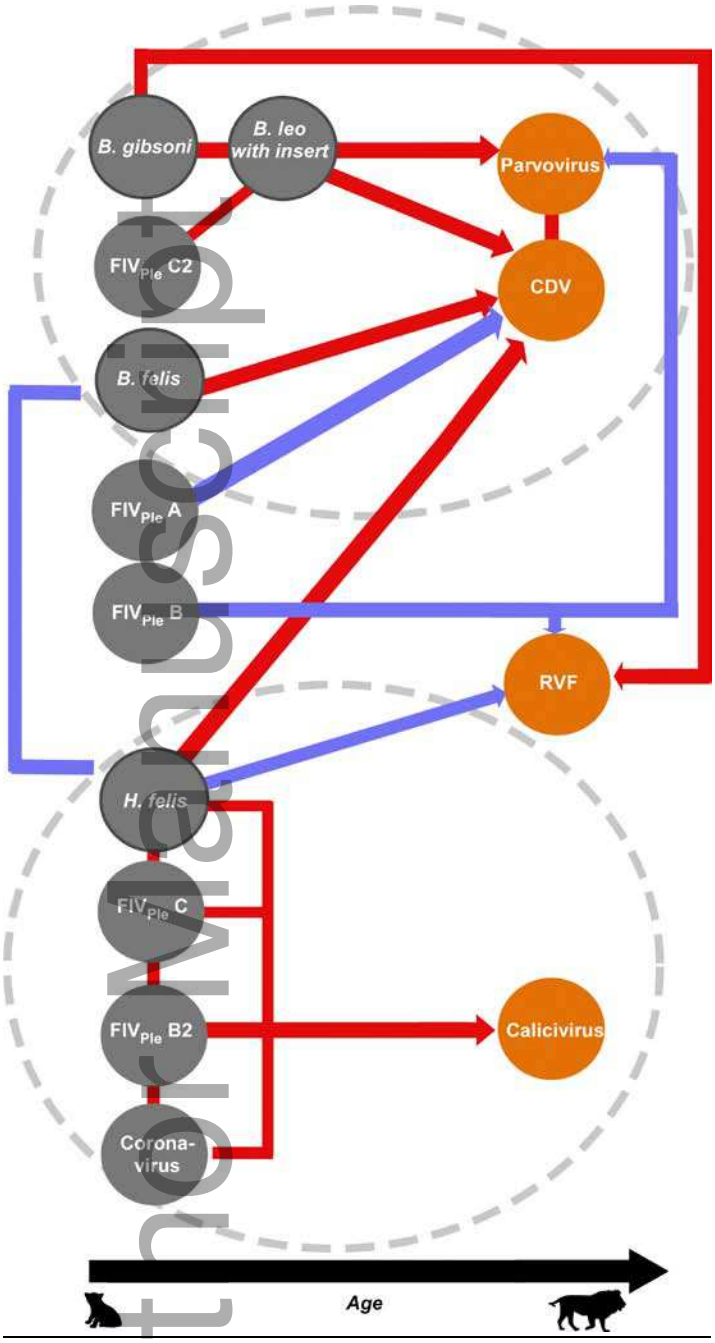

Fig. 3: Summary of the strong positive (red line/arrows) and negative (blue lines/arrows) associations between endemic (grey circles) and epidemic (orange circles) pathogens in the Serengeti lions; dark-grey borders indicate protozoa. The direction of the red or blue arrows indicates the potential sequence of infection events. The black arrow along the X-axis represents age; the circles reflect the ages when lions were likely to be infected by each pathogen (based on

703 age-exposure data rather than longitudinal data, see Fig. S1). Dashed circles indicate major co-
704 occurrence clusters identified at the landscape-year scale.

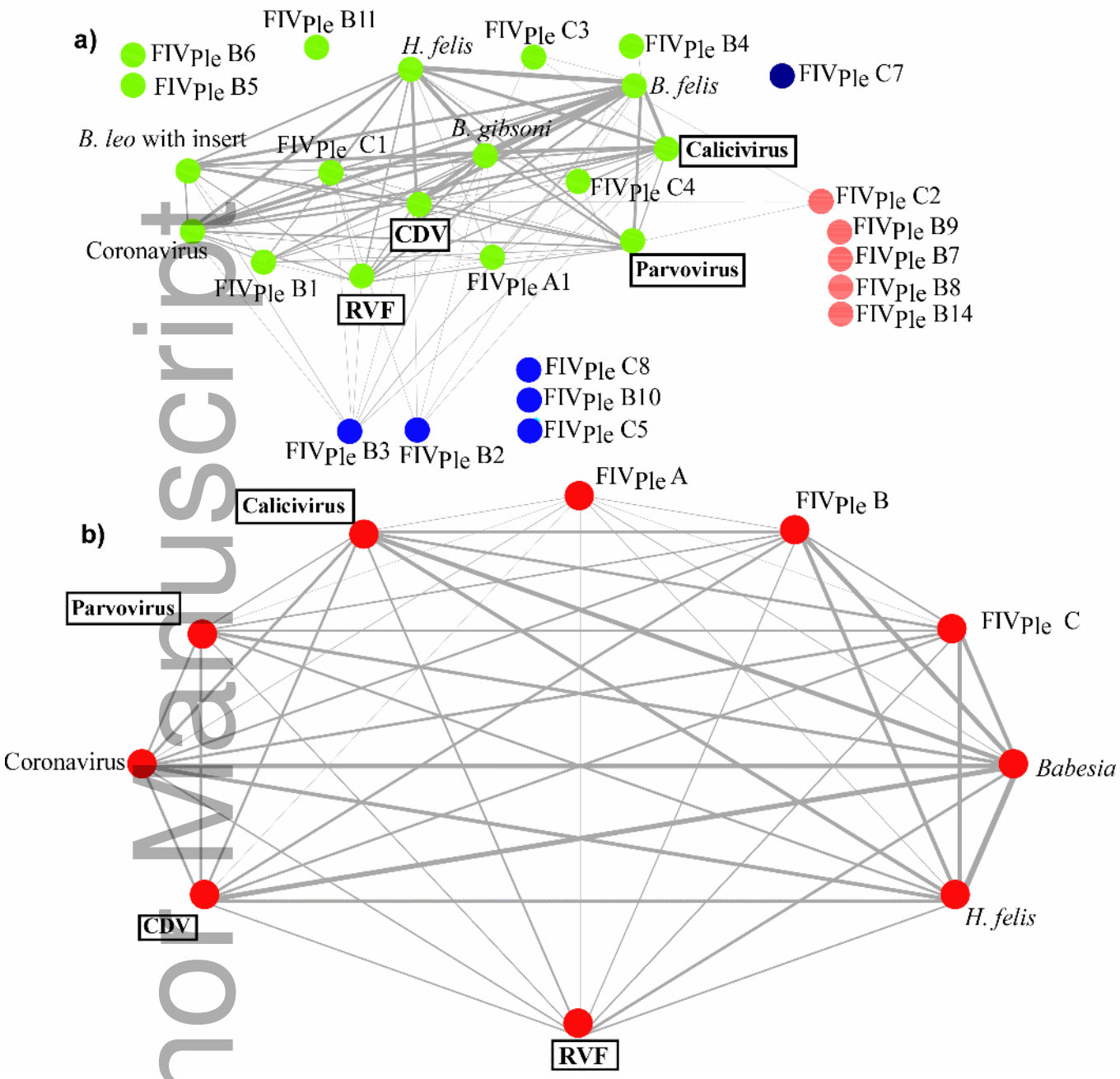

ele_13250_f1.tif

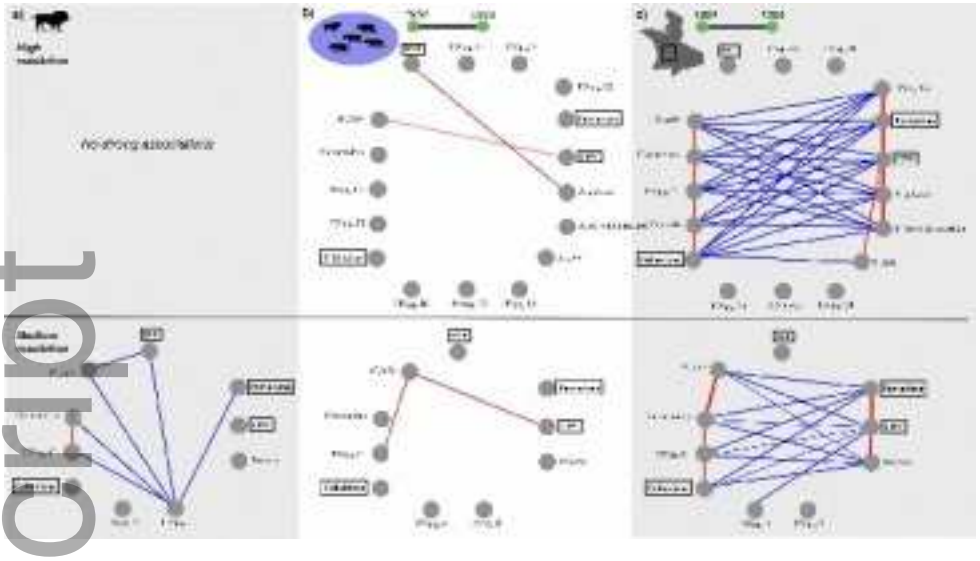

ele_13250_f2.tif

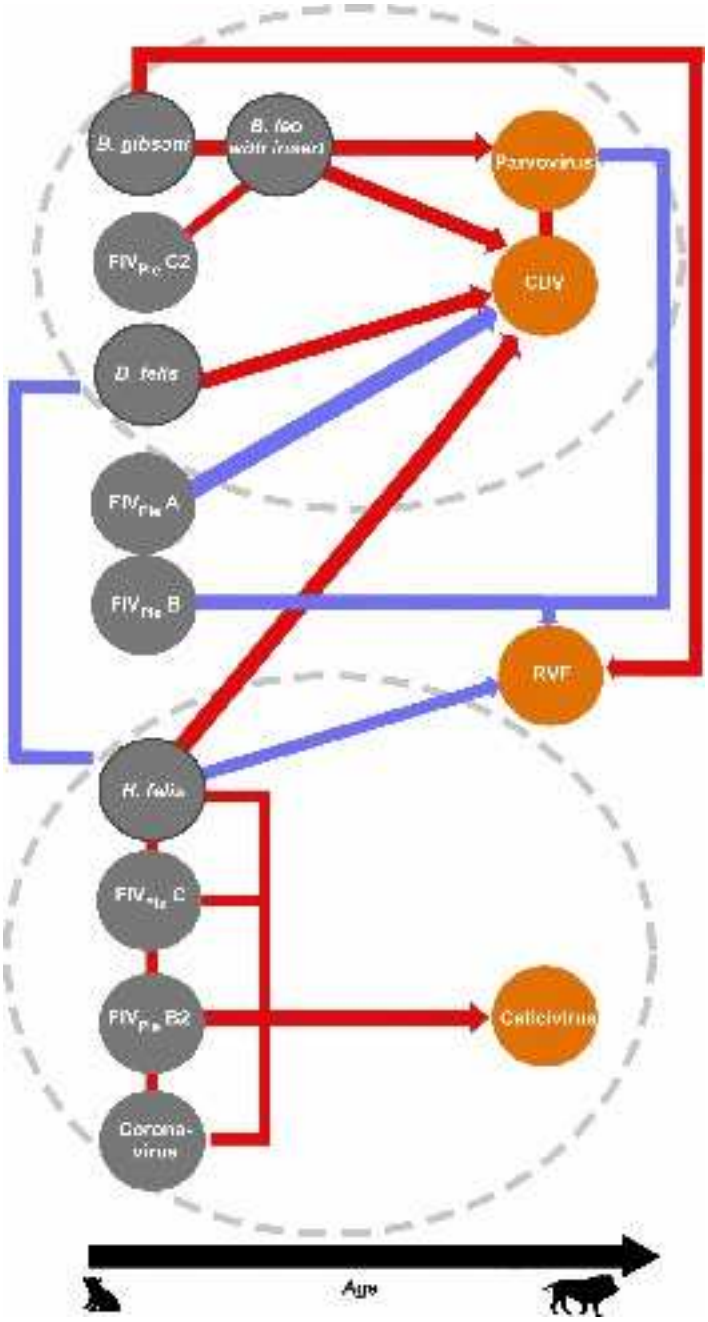

ele_13250_f3.tif